VNU Journal of Science: Mathematics – Physics, Vol. 40, No. 2 (2024) 79-90

VNU Journal of Science: Mathematics - Physics

Journal homepage: https://js.vnu.edu.vn/MaP

Original Article

Dynamic Analysis of Hexagon Honeycomb Sandwich Plate Resting on Elastic Foundations

Vu Minh Anh*, Tran Thanh Tung

VNU University of Engineering and Technology, 144 Xuan Thuy, Cau Giay, Hanoi, Vietnam

Received 7 December 2023
Revised 16 April 2024; Accepted 02 May 2024

Abstract: Dynamic analysis of hexagon honeycomb sandwich plate resting on elastic foundations are presented. Modeling is formed by 3 layers, in which core layer is hexagon honeyconb and facesheet layers is isotropic material. The Reddy's first order shear deformation plate theory and Galerken method are used to investigate the influnce of elastic foundations, geometrical parameters and material properties of hexagon honeycomb on the deflection – time curve. The value of the natural frequency was compared to the results reported in other works forevaluating the acuracy of used method.

Keywords: Dynamic analysis; sandwich plate; hexagon honeycomb; commposite material; elastic foundations.

1. Introduction

Materials with negative poisson coefficients have many outstanding properties such as mechanical properties and special designs such as: 2D auxetic, 3D auxetic, hexagon honeycomb, etc. Because of such outstanding properties, this material attracts the attention of researchers and manufacturers in recent years. Research is carried out using numerical and analytical methods such as Zang et al., [1] performed experiments to test compressive properties and failure mechanisms of materials reinforced by auxetic structures. To evaluate the contribution of auxetic core on the relationship between force and deflection of sandwich plate, the study are investigated by Yolcu and Baba [2]. Li et al., [3] proposed a new auxetic structure with mechanical properties that are determined by the finite element method and experiments. By using the first - order shear deformation theory, the vibration behavior and load capacity of sandwich plates with honeycomb auxetic core and porous materials facesheets are evaluated by Fu et al., [4]. Lieu

* Corresponding author.
E-mail address: vuminhanhhp@gmail.com

https//doi.org/10.25073/2588-1124/vnumap.4908

et al., [5] used the third – order shear deformation theory to investigated the influence of geometric characteristics of the honeycomb core layer on the static bending and buckling of nanobeams. A novel 3D hybrid auxetic-honeycomb lattice structures were developed by Hu et al., [6] to demonstrate that the compression resistance of the new structure is 84 – 122 times better than the corresponding structure. To solve the problem of low stiffness due to high porosity, Zhu et al., [7] proposed a new elliptical auxetic structure, the results indicated that a novel structure has a higher the average stress and absorption capacity.

Vibration plays an important role in structural evaluation and analysis because it represents the relationship between load and deflection. This evaluation provides important information about the working capacity and bearing capacity of structures subjected to loads such as wind, earthquake, and impact loads. To minimize peeling between the data board surface and the core layer, the authors of [8] used foam. Besides, the authors also evaluated the influence of foam on the mechanical properties of the auxetic structure. Zanjanchi et al., [9] used the first shear deformation plate theory to investigate the effect of elastic foundation, geometric parameter, temperature increment, distribution of CNTs on the nonlinear vibration of sandwich plate with auxetic honeycomb core. Liu et al., [10] considered the effective material properties of auxetic honeycombs with Gibson function and used analytical method to determine the response curves with the influnece of important parameters. The authors of [11] studied the auxetic beams reinforced by graphene origami layer reinforcement with distribution, weight fraction, variable thickness in fluid. Ni et al., [12] proposed a novel auxetic structure combined from three structures: original re-entrant hexagonal honeycomb and cross-chiral honeycomb. The novel structure has better stiffness and stability than the component materials. Burlayenko and Sadowski [13] used finite element code ABAQUS to investigate dynamic behavior of skin/core debonding on sandwich plates.

In this work we investigate the nonlinear vibration and dynamic of hexagon honeycomb sandwich plate resting on elastic foundation. The galerkin method and the first order shear theory are used to evaluate the influnce of geometrical parameter, elastic foundation, structure of hexagon honeycomb on the deflection - time curves.

2. Problem Statement

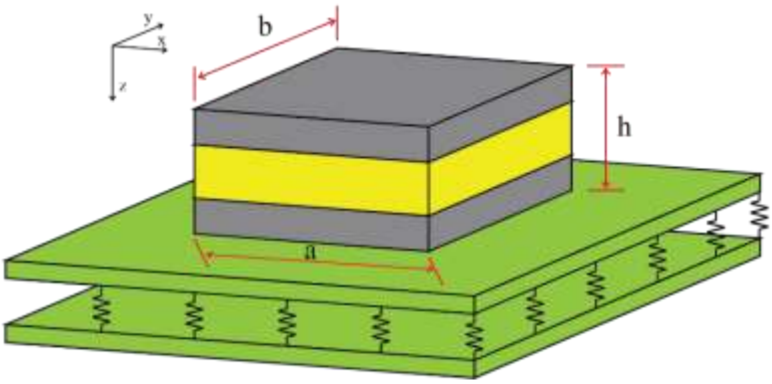

Figure 1. Modeling of the sandwich plate on Pasternak's elastic foundation.

Considering a sandwich plate composed of a hexagon honeycomb core layer and isotropic material face sheets in the xyz coordinate system with length a, width b, and thickness h. The xy plane is placed in the middle of the plate and the z-axis is set according to the thickness of the plate. The thickness of plate h is sum of the thickness of a core layer h_c and two face sheet layers h_f. Observing in Figure 1, qyer of plate with the hexagon honeycomb special shape made from isotropic homogeneous aluminum, the material properties are shown as:

$$
\begin{aligned}
&E_1^{(c)} = E_c\left(\frac{t_c}{l_c}\right)^3 \frac{\cos\theta_c}{(1+\sin\theta_c)\sin^2\theta_c}\left[1-\cot^2\theta_c\left(\frac{t_c}{l_c}\right)^2\right],\\
&E_2^{(c)} = E_c\left(\frac{t_c}{l_c}\right)^3 \frac{(1+\sin\theta_c)}{\cos^3\theta_c}\left[1-\left(\sec^2\theta_c+\tan^2\theta_c\right)\left(\frac{t_c}{l_c}\right)^2\right],\\
&G_{12}^{(c)} = G_c\left(\frac{t_c}{l_c}\right)^3 \frac{(1+\sin\theta_c)}{3\cos\theta_c},\\
&G_{13}^{(c)} = G_c\frac{t_c}{l_c}\frac{\cos\theta_c}{(1+\sin\theta_c)},\\
&G_{23}^{(c)} = \frac{1}{2}G_c\frac{t_c}{l_c}\left(\frac{1+\sin\theta_c}{2\cos\theta_c}+\frac{1+\sin^2\theta_c}{2(1+\sin\theta_c)\cos\theta_c}\right),\\
&\nu_{12}^{(c)} = \frac{\cos^2\theta_c}{(1+\sin\theta_c)\sin\theta_c}\left[1-\csc^2\theta_c\left(\frac{t_c}{l_c}\right)^2\right],\\
&\nu_{21}^{(c)} = \frac{(1+\sin\theta_c)\sin\theta_c}{\cos^2\theta_c}\left[1-2\sec^2\theta_c\left(\frac{t_c}{l_c}\right)^2\right],\\
&\rho^{(c)} = \rho_c\frac{t_c}{l_c}\frac{2}{(1+\sin\theta_c)\cos\theta_c}.
\end{aligned}
\tag{1}
$$

in which l_c and t_c are the cell wall length and call wall thickness.

The Young's modulus, Poisson's ratio, density and thermal expansion coefficient of material Aluminum with three types are shown in Table 1 [14].

Table 1. Mechanical properties of material Aluminum with three types

Material	PmPV	PMMA	Ti-6Al-4V
E (GPa)	$(3.51-0.0047T)$	$(3.52-0.0034T)$	$122.56(1-0.004568T)$
$\rho(Kg/m^3)$	1150	1150	4429
ν	0.3	0.34	0.29
α/K	$45(1+0.0005\Delta T)\times10^{-6}$	$45(1+0.0005\Delta T)\times10^{-6}$	$7.5788(6.638\times10^{-4}T-3.147\times10^{-6}T^2)$

3. Governing Equations

The force and moment resultants of the sandwich plate are defined as

$$\begin{aligned}
N_i &= \sum_{k=1}^{n} \int_{h_{k-1}}^{h_k} (\sigma_i)_k \, dz, i = x, y, xy, \\
M_i &= \sum_{k=1}^{n} \int_{h_{k-1}}^{h_k} (\sigma_i)_k \, zdz, i = x, y, xy, \\
Q_i &= K \sum_{k=1}^{n} \int_{h_{k-1}}^{h_k} (\sigma_i)_k \, dz, i = xz, yz.
\end{aligned} \tag{2}$$

The compatibility equation of the imperfect sandwich plate as

$$\begin{aligned}
&\left(N_x, N_y, N_{xy}\right) = \left(B_{11}, B_{12}, B_{16}\right)\varepsilon_x^0 + \left(B_{12}, B_{22}, B_{26}\right)\varepsilon_y^0 + \left(B_{16}, B_{26}, B_{66}\right)\gamma_{xy}^0 \\
&+\left(C_{11}, C_{12}, C_{16}\right)k_x + \left(C_{12}, C_{22}, C_{26}\right)k_y + \left(C_{16}, C_{26}, C_{66}\right)k_{xy} - \left(O_x^T, O_y^T, O_{xy}^T\right)\Delta T, \\
&\left(M_x, M_y, M_{xy}\right) = \left(C_{11}, C_{12}, C_{16}\right)\varepsilon_x^0 + \left(C_{12}, C_{22}, C_{26}\right)\varepsilon_y^0 + \left(C_{16}, C_{26}, C_{66}\right)\gamma_{xy}^0 \\
&+\left(E_{11}, E_{12}, E_{16}\right)k_x + \left(E_{12}, E_{22}, E_{26}\right)k_y + \left(E_{16}, E_{26}, E_{66}\right)k_{xy} - \left(N_x^T, N_y^T, N_{xy}^T\right)\Delta T, \\
&\left(Q_x, Q_y\right) = \left(I_{45}, I_{44}\right)\gamma_{yz} + \left(I_{55}, I_{45}\right)\gamma_{xz}.
\end{aligned} \tag{3}$$

where

$$\begin{aligned}
\varepsilon_x^0 &= B_{11}^* f_{,yy} + B_{12}^* f_{,xx} - B_{16}^* f_{,xy} + C_{11}^* k_x + C_{12}^* k_y + C_{16}^* k_{xy} + \Phi_1^T \Delta T, \\
\varepsilon_y^0 &= B_{12}^* f_{,yy} + B_{22}^* f_{,xx} - B_{26}^* f_{,xx} + C_{21}^* k_x + C_{22}^* k_y + C_{26}^* k_{xy} + \Phi_2^T \Delta T, \\
\gamma_{xy}^0 &= B_{16}^* f_{,yy} + B_{26}^* f_{,xx} - B_{66}^* f_{,xx} + C_{36}^* k_x + B_{46}^* k_y + C_{66}^* k_{xy} + \Phi^T \Delta T.
\end{aligned} \tag{4}$$

The motion equations for the sandwich plats are

$$\begin{aligned}
&M_{11}(w) + M_{12}(\phi_x) + M_{13}(\phi_y) + Q_1(w, f) \\
&\qquad\qquad + M_{11}(w^*) + M_{14}(w^*, f) + q = \text{¡}_0 \frac{\partial^2 w}{\partial t^2}, \\
&M_{21}(w) + M_{22}(\phi_x) + M_{23}\left(\phi_y\right) + M_{24}(f) + M_{21}(w^*) = \left(\text{¡}_2 - \frac{\text{¡}_1^2}{\text{¡}_0}\right)\frac{\partial^2 \phi_x}{\partial t^2}, \\
&M_{31}(w) + M_{32}(\phi_x) + M_{33}\left(\phi_y\right) + M_{34}(f) + M_{31}(w^*) = \left(\text{¡}_2 - \frac{\text{¡}_1^2}{\text{¡}_0}\right)\frac{\partial^2 \phi_y}{\partial t^2}.
\end{aligned} \tag{5}$$

in which the parameters $M_{1i}, M_{2i}, M_{3i}\ (i = \overline{1,4}), \text{¡}_0, \text{¡}_1, \text{¡}_2$ are expressed in Appendix A.

The compatibility equation of the imperfect sandwich plate as

$$\begin{aligned}
&B_{11}^* f_{,yyyy} + \left(2B_{12}^* + B_{66}^*\right) f_{,xxyy} - 2B_{16}^* f_{,xyyy} - 2B_{26}^* f_{,xxxy} + B_{22}^* f_{,xxxx} \\
&+\left(C_{11}^* - C_{66}^*\right)\phi_{x,xyy} + C_{16}^*\phi_{x,yyy} + C_{21}^*\phi_{x,xxx} + \left(C_{26}^* - C_{36}^*\right)\phi_{x,xxy} \\
&+C_{12}^*\phi_{y,yyy} + \left(C_{16}^* - C_{46}^*\right)\phi_{y,xyy} + \left(C_{22}^* - C_{66}^*\right)\phi_{y,xxy} + C_{26}^*\phi_{y,xxx} \\
&= w_{,xy}^2 - w_{,xx}w_{,yy} + 2w_{,xy}w_{,xy}^* - w_{,xx}w_{,yy}^* - w_{,yy}w_{,xx}^*.
\end{aligned} \tag{6}$$

in which

$$\begin{aligned}
&B_{11}^{*} f_{,yyyy} + \left(2B_{12}^{*} + B_{66}^{*}\right) f_{,xxyy} - 2B_{16}^{*} f_{,xyyy} - 2B_{26}^{*} f_{,xxxy} + B_{22}^{*} f_{,xxxx} \\
&+\left(C_{11}^{*} - C_{66}^{*}\right)\phi_{x,xyy} + C_{16}^{*}\phi_{x,yyy} + C_{21}^{*}\phi_{x,xxx} + \left(C_{26}^{*} - C_{36}^{*}\right)\phi_{x,xxy} \\
&+C_{12}^{*}\phi_{y,yyy} + \left(C_{16}^{*} - C_{46}^{*}\right)\phi_{y,xyy} + \left(C_{22}^{*} - C_{66}^{*}\right)\phi_{y,xxy} + C_{26}^{*}\phi_{y,xxx} \\
&= w_{,xy}^{2} - w_{,xx}w_{,yy} + 2w_{,xy}w_{,xy}^{*} - w_{,xx}w_{,yy}^{*} - w_{,yy}w_{,xx}^{*}.
\end{aligned} \tag{7}$$

$$\begin{aligned}
&C_{11}^{*} = -\left(c_2e_3 - e_2c_3\right)/\Delta, C_{12}^{*} = -\left(c_2e_4 - e_2c_4\right)/\Delta, C_{16}^{*} = -\left(c_2e_5 - e_2c_5\right)/\Delta \\
&C_{21}^{*} = \left(c_1e_3 - e_1c_3\right)/\Delta, C_{22}^{*} = \left(c_1e_4 - e_1c_4\right)/\Delta, C_{26}^{*} = \left(c_1e_5 - e_1c_5\right)/\Delta \\
&C_{36}^{*} = \left(-B_{16}C_{11}^{*} - A_{26}C_{21}^{*} - C_{16}\right)/B_{66}, C_{46}^{*} = \left(-B_{16}C_{12}^{*} - A_{26}C_{22}^{*} - C_{26}\right)/B_{66} \\
&C_{66}^{*} = \left(-B_{16}C_{16}^{*} - A_{26}C_{26}^{*} - C_{66}\right)/B_{66}
\end{aligned}$$

The boundary conditions assume that the four edges of the imperfect sandwich plate are simply supported as

$$\begin{aligned}
&w = N_{xy} = M_x = 0, N_x = N_x^0 \quad at \quad x = 0, a, \\
&w = N_{xy} = M_y = 0,\ N_y = N_y^0 \quad at \quad y = 0, b.
\end{aligned} \tag{8}$$

The problem's solutions consist of a double trigonometric function that meets the given boundary condition as follows

$$\begin{Bmatrix} w(x,y,t) \\ w^{*}(x,y,t) \\ \phi_x(x,y,t) \\ \phi_y(x,y,t) \end{Bmatrix} = \begin{pmatrix} W(t) & 0 & 0 & 0 \\ 0 & W_0 = \mu h & 0 & 0 \\ 0 & 0 & \Phi_x(t) & 0 \\ 0 & 0 & 0 & \Phi_y(t) \end{pmatrix} \begin{Bmatrix} \sin\lambda_m x \sin\delta_n y \\ \sin\lambda_m x \sin\delta_n y \\ \cos\lambda_m x \sin\delta_n y \\ \sin\lambda_m x \cos\delta_n y \end{Bmatrix}. \tag{9}$$

$$\begin{aligned}
&f(x,y,t) = T_1(t)\cos 2\lambda_m x + T_2(t)\cos 2\delta_n y + T_3(t)\sin\lambda_m x \sin\delta_n y \\
&+T_4(t)\cos\lambda_m x\cos\delta_n y + \frac{1}{2}N_{x0}y^2 + \frac{1}{2}N_{y0}x^2.
\end{aligned} \tag{10}$$

where

$$\begin{aligned}
&T_1 = \frac{1}{32}\frac{\delta_n^{\,2}}{A_{22}^{*}\lambda_m^{\,2}}W\left(W + 2W_0\right), T_2 = \frac{1}{32}\frac{\lambda_m^{\,2}}{A_{11}^{*}\delta_n^{\,2}}W\left(W + 2W_0\right), \\
&T_3 = T_3^1\Phi_x + T_3^2\Phi_y, T_4 = T_4^1\Phi_x + T_4^2\Phi_y. \\
&T_3^1 = \frac{\left(\Upsilon_3\Upsilon_1 - \Upsilon_5\Upsilon_2\right)}{\Upsilon_2^{\,2} - \Upsilon_1^{\,2}}, T_3^2 = \frac{\left(\Upsilon_4\Upsilon_1 - \Upsilon_6\Upsilon_2\right)}{E^2 - \Upsilon_1^{\,2}}, \\
&T_4^1 = \frac{\left(\Upsilon_5\Upsilon_1 - \Upsilon_3\Upsilon_2\right)}{\Upsilon_2^{\,2} - \Upsilon_1^{\,2}}, T_4^2 = \frac{\left(\Upsilon_6\Upsilon_1 - \Upsilon_4\Upsilon_2\right)}{E^2 - \Upsilon_1^{\,2}}.
\end{aligned} \tag{11}$$

with

$$\begin{aligned}
&\Upsilon_1 = \left[B_{11}^{*}\delta_n^{\,4} + \left(2B_{12}^{*} + B_{66}^{*}\right)\lambda_m^{\,2}\delta_n^{\,2} + B_{22}^{*}\lambda_m^{\,4}\right], \Upsilon_2 = \left(2B_{16}^{*}\lambda_m\delta_n^{\,3} + 2B_{26}^{*}\lambda_m^{\,3}\delta_n\right), \\
&\Upsilon_3 = \left[\left(C_{11}^{*} - C_{66}^{*}\right)\lambda_m\delta_n^{\,2} + C_{21}^{*}\lambda_m^{\,3}\right], \Upsilon_4 = \left[C_{12}^{*}\delta_n^{\,3} + \left(C_{22}^{*} - C_{66}^{*}\right)\lambda_m^{\,2}\delta_n\right], \\
&\Upsilon_5 = \left[-C_{16}^{*}\delta_n^{\,3} - \left(C_{26}^{*} - C_{36}^{*}\right)\lambda_m^{\,2}\delta_n\right], \Upsilon_6 = \left[-\left(C_{16}^{*} - C_{46}^{*}\right)\lambda_m\delta_n^{\,2} - C_{26}^{*}\lambda_m^{\,3}\right].
\end{aligned}$$

Applying the Bubnov - Galerkin method to Eq. (5) after replacing Eq. (9) results in

$$\begin{aligned}
&\left[m_{11}-\left(N_{x0}\lambda_m{}^2+N_{y0}\delta_n{}^2\right)\right]W+m_{12}\Phi_x+m_{13}\Phi_y+m_{14}\left(W+W_0\right)\Phi_x \\
&+m_{15}\left(W+W_0\right)\Phi_y+m_{16}W_0+m_{17}W\left(W+W_0\right)\left(W+2W_0\right)+m_{18}q=\rho_0\frac{\partial^2 \mathrm{W}}{\partial t^2}, \\
&m_{21}W+m_{22}\Phi_x+m_{23}\Phi_y+m_{24}W\left(W+2W_0\right)+m_{25}W_0=\left(\rho_2-\frac{\rho_1{}^2}{\rho_0}\right)\frac{\partial^2\Phi_x}{\partial t^2}, \\
&m_{31}W+m_{32}\Phi_x+m_{33}\Phi_y+m_{34}W\left(W+2W_0\right)+m_{35}W_0=\left(\rho_2-\frac{\rho_1{}^2}{\rho_0}\right)\frac{\partial^2\Phi_y}{\partial t^2}.
\end{aligned} \tag{12}$$

where the detail of coefficients $m_{1i}(i=\overline{1,8}), \mathrm{m}_{jk}(j=\overline{2,3}, k=\overline{1,5})$ may be found in Appendix B.

The reaction forces on two sides $y=0,b$ is determined as

$$\begin{aligned}
&\left[m_{11}+\left(P_y\lambda_m{}^2+P_x\delta_n{}^2\right)h\right]W+m_{12}\Phi_x+m_{13}\Phi_y+m_{14}\left(W+W_0\right)\Phi_x \\
&+m_{15}\left(W+W_0\right)\Phi_y+m_{16}W_0+m_{17}W\left(W+W_0\right)\left(W+2W_0\right)+m_{18}q=\rho_0\frac{\partial^2 \mathrm{W}}{\partial t^2}, \\
&m_{21}W+m_{22}\Phi_x+m_{23}\Phi_y+m_{24}W\left(W+2W_0\right)+m_{25}W_0=\left(\rho_2-\frac{\rho_1{}^2}{\rho_0}\right)\frac{\partial^2\Phi_x}{\partial t^2}, \\
&m_{31}W+m_{32}\Phi_x+m_{33}\Phi_y+m_{34}W\left(W+2W_0\right)+m_{35}W_0=\left(\rho_2-\frac{\rho_1{}^2}{\rho_0}\right)\frac{\partial^2\Phi_y}{\partial t^2}.
\end{aligned} \tag{13}$$

In order to obtain the natural frequencies, the system equations (15) are used with $q=0$

$$\begin{bmatrix} m_{11}+I_0\omega^2 & m_{12} & m_{13} \\ m_{21} & m_{22}+\rho_1\omega^2 & m_{23} \\ m_{31} & m_{32} & m_{33}+\rho_1\omega^2 \end{bmatrix}=0 \tag{14}$$

4. Discussion

To evaluate the accuracy of the method used, the value of the natural oscillation frequency was compared with the results of another similar paper. Table 2 is the result of comparing the dimensionless frequency with the results reported in [16]. The compared results indicated that the used methodology in this work is completely appropriate.

Table 2. Comparison of the natural frequencies of isotropic plate

		$(a/b=2\,;\,h/a=1/12)$		$(a/b=2\,;\,h/a=1/20)$	
		Farsangi et al., [15]	Present	Farsangi et al., [15]	Present
(m,n)	(1,1)	0.1576	0.1563	0.0589	0.0563
	(2,1)	0.2444	0.2409	0.930	0.0867
	(3,1)	0.3788	0.3977	0.1481	0.1432
	(4,1)	0.5497	0.6253	0.2218	0.2251

In order to evaluate the effect of geometrical parameter, elastic foundation, structure of hexagon honeycomb on the deflection – time curves, the titanium alloy (Ti-6Al-4V) is chosen. Table 3 shows the effect of mode (m,n) and elastic foundations on the natural frequencies of sandwich plate. As can see that the mode (m,n) and elastic foundations have a positive influence. The natural frequencies increase when mode (m,n) and elastic foundations increase.

Table 3. The natural frequencies of sandwich plate with the influnce of mode (m,n) and elastic foundations

$(k_1,k_2)(GPa/m;GPa.m)$	(m,n)					
	(1,1)	(1,2)	(1,3)	(3,1)	(3,3)	(5,5)
0,0	1050.62	2585.41	5043.47	5053.65	8766.17	21635.5
0,2;0,02	1476.4	2969.52	5413.78	5423.21	9135.15	22030.2
0,2;0,04	1701.15	3254.58	5729.32	5738.18	9471.23	22410.3
0,5;0.05	1947.73	3466.79	5926.01	5934.54	9662.23	22609.3

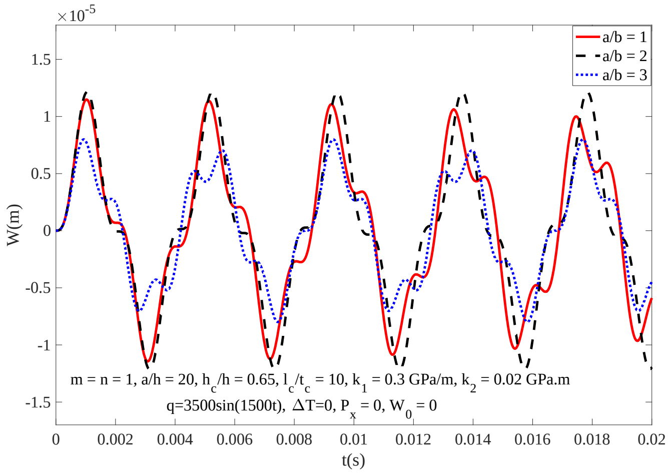

Figure 2. Effect of the a/b ratio on the time - deflection curves.

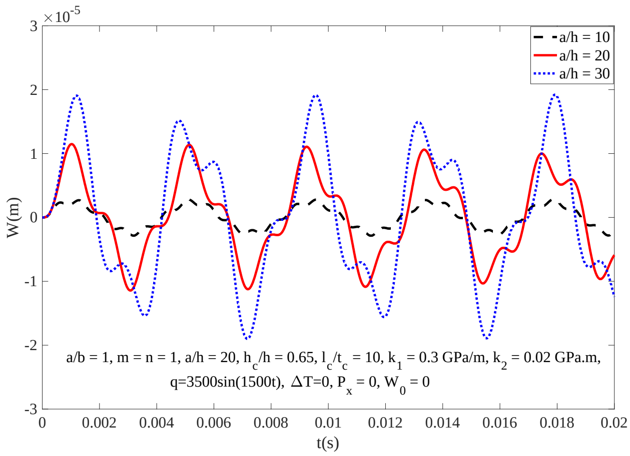

Figure 3. Effect of the a/h ratio on the time - deflection curves.

Figs. 2 and 3 show the impact of a/b ratio and a/h ratio on deflection - time curves of sandwich plate. In Fig. 2, three values of a/b ratio (1, 2, 3) are considered. It is evident that as the a/b ratio increases, the amplitude deflection also increases. This it can be shown that the a/b ratio has a negative effect. The effect assessment of the a/h ratio in the Fig. 3 similar with the a/b ratio.

To explore the nonlinear vibration of the plate with the influence of the geometric characteristics of the hexagonal honeycomb core layer, the influence of l_c/t_c ratio on the deflection – time curves of the sandwich plate in Fig. 4. It can be see that the deflection amplitude uptrends when the lc/tc ratio increases. This behavior is explained because increasing the l_c/t_c ratio leads to the unit cells of the hexagonal honeycomb core larger, in other words the wall thickness of the hexagonal edge smaller.

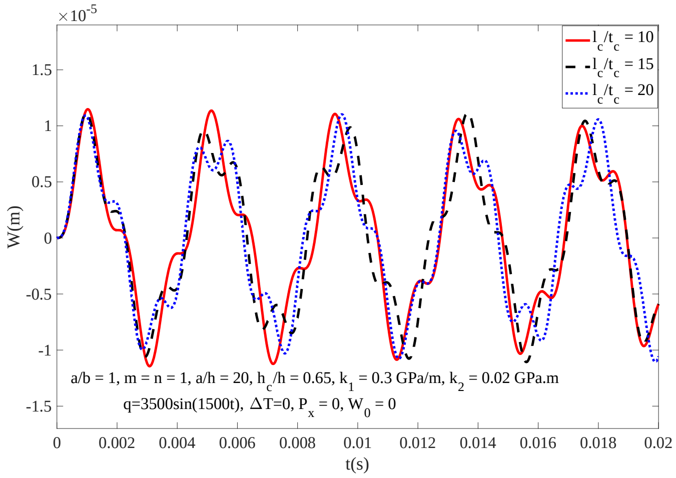

Figure 4. Effect of l_c/t_c ratio on the time - deflection curves.

Besides, the influence of the honeycomb characteristic angle on the time - deflection curves of the sandwich plate are plotted in Fig. 5. It can be observed that the deflection amplitude reduces when the honeycomb characteristic angle decreases.

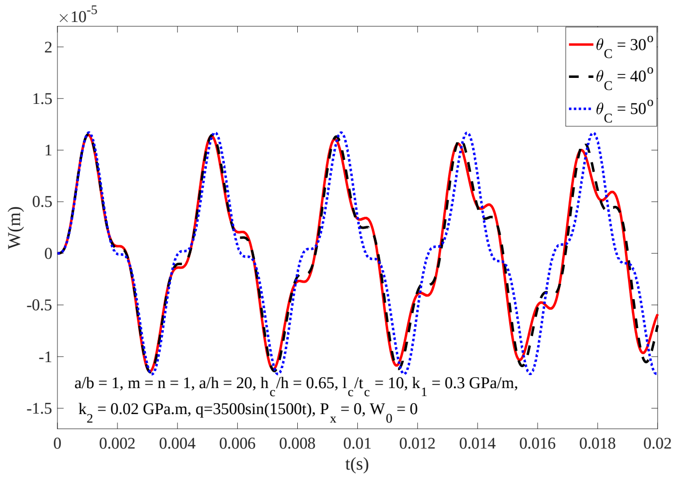

Figure 5. Effect of the honeycomb characteristic angle on the deflection – time curves of the sandwich plate.

Figs. 6 and 7 display the effect of the Winkler and Pasternak foudation on the deflection – time curves on the sandwich plate. The value of Winkler and Pasternak foudation have positive effect on the decreasing the deflection amplitude. This behavior can explained by elastic foundation is considered as reinforcement layer with aim improve mechanical strength results in enhancement load – carrying capability of sandwich plate.

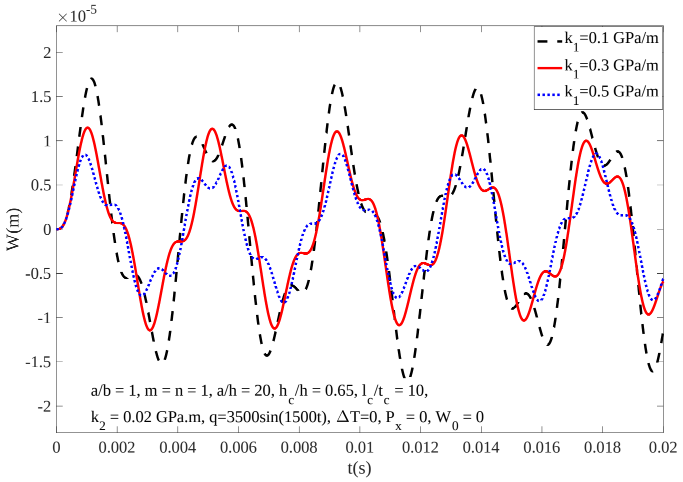

Figure 6. Effect of Winkler foundtion on the time - deflection curves.

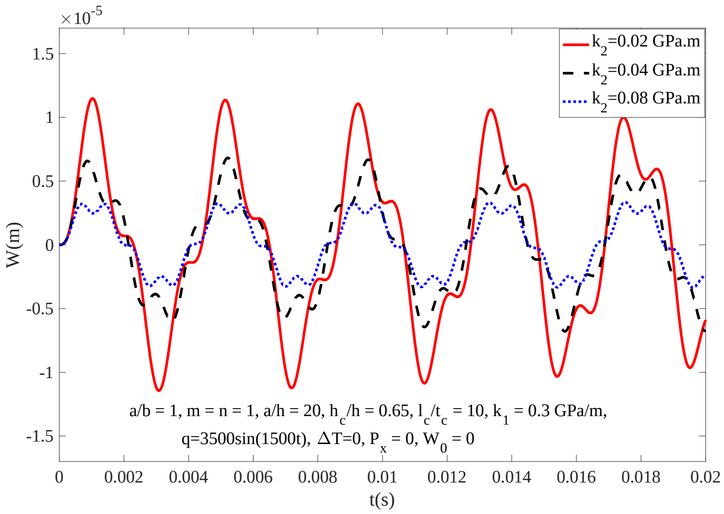

Figure 7. Effect of Pasternak foundtion on the time - deflection curves.

5. Conclusions

In this work we investigated the nonlinear vibration and dynamic of hexagon honeycomb sandwich plate resting on elastic foundation. The galerkin method and the first order shear theory were used to evaluate the influnce of geometrical parameter, elastic foundation, structure of hexagon honeycomb on the deflection – time curves. Some outstanding results as:

- The accuracy of used method is verified with the results of previously published papers.
- The fluctuation amplitude of sandwich plate reduced if sandwich plate was reinforced by elastic foundation.
- The structure of core layer is evaluated in details with teta and lc/tc.
- The geometric parameters have a substantial influence on the time - deflection curves.

Acknowledgments

This research is funded by the Project number CN.22.16 of VNU Hanoi – University of Engineering and Technology. The authors are grateful for this support.

References

[1] X. Zang, X. Zheng, L. Song, Y. Tian, Compressive Properties and Failure Mechanisms of 3D-Printed Continuous Carbon Fiber-Reinforced Auxetic Structures, Composites Communications, Vol. 43, 2023, pp. 101744, https://doi.org/10.1016/j.coco.2023.101744.

[2] D. A. Yolcu, B. O. Baba, Experimental Investigation on Impact Behavior of Curved Sandwich Composites with Chiral Auxetic Core, Composite Structures, Vol. 329, No. 1, 2024, pp. 117749, https://doi.org/10.1016/j.compstruct.2023.117749.

[3] N. Li, S. Liu, X. Wu, J. Wang, Y. Han, X. Zhang, Mechanical Characteristics of A Novel Rotating Star-Rhombic Auxetic Structure with Multi-Plateau Stages, Thin-Walled Structures, Vol. 191, 2023, pp. 111081, https://doi.org/10.1016/j.tws.2023.111081.

[4] T. Fu, X. Hu, C. Yang, Impact Response Analysis of Stiffened Sandwich Functionally Graded Porous Materials Doubly-Curved Shell with Re-Entrant Honeycomb Auxetic Core, Applied Mathematical Modelling, Vol. 124, 2023, pp. 553-575, https://doi.org/10.1016/j.apm.2023.08.024.

[5] P. V. Lieu, A. M. Zenkour, G. T. Luu, Static Bending and Buckling of FG Sandwich Nanobeams with Auxetic Honeycomb Core, European Journal of Mechanics - A/Solids, Vol. 103, 2024, pp. 105181, https://doi.org/10.1016/j.euromechsol.2023.105181.

[6] Q. Hu, G. Lu, K. M. Tse, Compressive and Tensile Behaviours of 3D Hybrid Auxetic-Honeycomb Lattice Structures, International Journal of Mechanical Sciences, Vol. 17, 2023, pp. 108767, https://doi.org/10.1016/j.ijmecsci.2023.108767.

[7] D. Zhu, Y. Wei, X. Shen, K. Yan, M. Yuan, S. Qi, A Novel Elliptical Annular Re-Entrant Auxetic Honeycomb with Enhanced Stiffness, International Journal of Mechanical Sciences, Vol. 9, 2023, pp. 108732, https://doi.org/10.1016/j.ijmecsci.2023.108732.

[8] V. N. Burlayenko, T. Sadowski, Analysis of Structural Performance of Sandwich Plates with Foam-Filled Aluminum Hexagonal Honeycomb Core, Computational Materials Science, Vol. 45, 2009, pp. 658-662, https://doi.org/10.1016/j.commatsci.2008.08.018.

[9] M. Zanjanchi, M. Ghadiri, S. S. Shomi, Nonlinear Parametric Excitation and Dynamic Stability of Auxetic Honeycombs Core with CNTRC Face Sheets Sandwich Plate, European Journal of Mechanics - A/Solids, Vol. 102, 2023, pp. 105109, https://doi.org/10.1016/j.euromechsol.2023.105109.

[10] Y. Liu, Z. Qin, F. Chu, Nonlinear Vibrations of Auxetic Honeycomb Thin Plates Based on the Modified Gibson Functions, Thin-Walled Structures, Vol. 193, 2023, pp. 111259, https://doi.org/10.1016/j.tws.2023.111259.

[11] B. Murari, S. Zhao, Y. Zhang, J. Yang, Static and Dynamic Instability of Functionally Graded Graphene Origami-Enabled Auxetic Metamaterial Beams with Variable Thickness in Fluid, Ocean Engineering, Vol. 280, No. 15, 2023, pp. 114859, https://doi.org/10.1016/j.oceaneng.2023.114859.

[12] X. H. Ni, W. Jiang, X. G. Zhang, D. Han, X. C. Teng, J. Hao, H. H. Xu, X. Ren, Quasi-static and Dynamic Properties Studies of A Metamaterial with Enhanced Auxeticity and Tunable Stiffness, Composite Structures, Vol. 321, No. 1, 2023, pp. 117254, https://doi.org/10.1016/j.compstruct.2023.117254.

[13] V. N. Burlayenko, T. Sadowski, Influence of Skin/Core Debondingo Free Vibration Behavior of Foam and Honeycomb Cored Sandwich Plates, International Journal of Non-Linear Mechanics, Vol. 45, 2010, pp. 959-968, https://doi.org/10.1016/j.ijnonlinmec.2009.07.002.
[14] N. D. Dat, N. V. Thanh, V. M. Anh, N. D. Duc, Vibration and Nonlinear Dynamic Analysis of Sandwich FG-CNTRC Plate with Porous Core Layer, Mechanics of Advanced Materials and Structures, Vol. 29, 2020, pp. 1431-1448, https://doi.org/10.1080/15376494.2020.1822476.
[15] M. A. Farsangi, A. R. Saidi, R. C. Batra, Analytical Solution for Free Vibrations of Moderately Thick Hybrid Piezoelectric Laminated Plates, Journal of Sound and Vibration, Vol. 332, No. 28, 2013, pp. 5981-5998, https://doi.org/10.1016/j.jsv.2013.05.010.

Appendixes

Appendix A

$$M_{11}\left(w\right)=2I_{45}w_{,xy}+I_{55}w_{,xx}+I_{44}w_{,yy}-k_1w+k_2\left(w_{,xx}+w_{,yy}\right)$$
$$M_{12}\left(\phi_x\right)=I_{55}\phi_{x.x}+I_{45}\phi_{x,y}$$
$$M_{13}\left(\phi_y\right)=I_{45}\phi_{y,x}+I_{44}\phi_{y,y}$$
$$M_{14}\left(w,f\right)=f_{,yy}w_{,xx}-2f_{,xy}w_{,xy}+f_{,xx}w_{,yy}$$

$$M_{21}\left(w\right)=-I_{55}w_{,x}-I_{45}w_{,y}$$
$$M_{22}\left(\phi_x\right)=L_{14}\phi_{x,xx}+\left(L_{16}+L_{34}\right)\phi_{x,xy}+L_{36}\phi_{x,yy}-I_{55}\phi_x$$
$$M_{23}\left(\phi_y\right)=L_{35}\phi_{y,yy}+L_{16}\phi_{y,xx}+\left(L_{36}+L_{15}\right)\phi_{y,xy}-I_{45}\phi_y$$
$$M_{24}\left(f\right)=L_{11}f_{,xyy}+L_{12}f_{,xxx}+L_{13}f_{,xxy}+L_{31}f_{,yyy}+L_{32}f_{,xxy}+L_{33}f_{,xyy}$$

$$M_{31}\left(w\right)=-I_{45}w_{,x}-I_{44}w_{,y}$$
$$M_{32}\left(\phi_x\right)=\left(L_{24}+L_{36}\right)\phi_{x,xy}+L_{26}\phi_{x,yy}+L_{34}\phi_{x,xx}-I_{45}\phi_x$$
$$M_{33}\left(\phi_y\right)=L_{25}\phi_{y,yy}+\left(L_{26}+L_{35}\right)\phi_{y,xy}+L_{36}\phi_{y,xx}-I_{44}\phi_y$$
$$M_{34}\left(f\right)=L_{21}f_{,yyy}+L_{22}f_{,xxy}+L_{23}f_{,xyy}+L_{31}f_{,xyy}+L_{32}f_{,xxx}+L_{33}f_{,xxy}$$

Appendix B

$$m_{11}=-I_{55}\lambda_m{}^2-I_{44}\delta_n{}^2-k_1-k_2\left(\lambda_m{}^2+\delta_n{}^2\right),m_{12}=-I_{55}\lambda_m,$$
$$m_{13}=-I_{44}\delta_n,m_{14}=\frac{32}{3mn\pi^2}\lambda_m{}^2\delta_n{}^2T_3^1,$$
$$m_{15}=\frac{32}{3mn\pi^2}\lambda_m{}^2\delta_n{}^2T_3^2,$$
$$m_{16}=-I_{55}\lambda_m{}^2-I_{44}\delta_n{}^2-k_1-k_2\left(\lambda_m{}^2+\delta_n{}^2\right),$$
$$m_{17}=-\frac{1}{16}\frac{\delta_n{}^4}{B_{22}^*}-\frac{1}{16}\frac{\lambda_m{}^4}{B_{11}^*},m_{18}=\frac{16}{mn\pi^2},$$

$$m_{21} = -I_{55}\lambda_m, m_{25} = -I_{55}\lambda_m,$$

$$m_{22} = \left(-L_{14}\lambda_m^2 - L_{36}\delta_n^2 - I_{55}\right) + \left[-\left(L_{11} + L_{33}\right)\lambda_m\delta_n{}^2 - L_{12}\lambda_m{}^3\right]T_3^1$$
$$+\left[\left(L_{13} + L_{32}\right)\lambda_m{}^2\delta_n + L_{31}\delta_n{}^3\right]T_4^1,$$

$$m_{23} = -\left(L_{36} + L_{15}\right)\lambda_m\delta_n + \left[-\left(L_{11} + L_{33}\right)\lambda_m\delta_n{}^2 - L_{12}\lambda_m{}^3\right]T_3^2$$
$$+\left[\left(L_{13} + L_{32}\right)\lambda_m{}^2\delta_n + L_{31}\delta_n{}^3\right]T_4^2,$$

$$m_{24} = \frac{8}{3}\frac{\lambda_m\delta_n}{mn\pi^2}\left(\frac{L_{12}}{B_{22}^*}\delta_n + \frac{L_{31}}{B_{11}^*}\lambda_m\right),$$

$$m_{31} = -I_{44}\delta_n, m_{35} = -I_{44}\delta_n$$

$$m_{32} = -\left(L_{24} + L_{36}\right)\lambda_m\delta_n + \left(-\left(L_{22} + L_{33}\right)\lambda_m{}^2\delta_n - L_{21}\delta_n{}^3\right)T_3^1$$
$$+\left[\left(L_{23} + L_{31}\right)\lambda_m\delta_n{}^2 + L_{32}\lambda_m{}^3\right]T_4^1$$

$$m_{33} = -L_{36}\lambda_m^2 - I_{44} - L_{25}\delta_n{}^2 + \left(-\left(L_{22} + L_{33}\right)\lambda_m{}^2\delta_n - L_{21}\delta_n{}^3\right)T_3^2$$
$$+\left[\left(L_{23} + L_{31}\right)\lambda_m\delta_n{}^2 + L_{32}\lambda_m{}^3\right]T_4^2$$

$$m_{34} = \frac{8}{3}\frac{\lambda_m\delta_n}{mn\pi^2}\left(\frac{L_{21}}{B_{11}^*}\lambda_m + \frac{L_{32}}{B_{22}^*}\delta_n\right)$$